Two-frequency Jahn-Teller systems in circuit QED

Tekin Dereli,[1] Yusuf Gül,[1] Pol Forn-Díaz,[2] and Özgür E. Müstecaplıoğlu[1,*]
[1]*Department of Physics, Koç University, Sarıyer, Istanbul, 34450, Turkey*
[2]*Norman Bridge Laboratory of Physics, California Institute of Technology, Pasadena, CA 91125, USA*
(Received 6 September 2011; published 30 May 2012)

We investigate the simulation of Jahn-Teller models with two nondegenerate vibrational modes using a circuit QED architecture. Typical Jahn-Teller systems are anisotropic and require at least a two-frequency description. The proposed simulator consists of two superconducting lumped-element resonators interacting with a common flux qubit in the ultrastrong coupling regime. We translate the circuit QED model of the system to a two-frequency Jahn-Teller Hamiltonian and calculate its energy eigenvalues and the emission spectrum of the cavities. It is shown that the system can be systematically tuned to an effective single-mode Hamiltonian from the two-mode model by varying the coupling strength between the resonators. The flexibility in manipulating the parameters of the circuit QED simulator permits the isolation of the effective single-frequency and pure two-frequency effects in the spectral response of Jahn-Teller systems.

DOI: 10.1103/PhysRevA.85.053841 PACS number(s): 42.50.Pq, 71.70.Ej, 85.25.−j

I. INTRODUCTION

Simulating complex physical phenomena using systems that offer precise control of physical interactions, such as ultracold atoms [1], Bose-Einstein condensates [2,3], and trapped ions [4], has attracted much attention in the last decade. It has recently been shown that cavity QED systems can be utilized for the same purpose, in particular to simulate certain gauge potentials, the anomalous Hall effect, and the Dirac equation [5]. The potential use of cavity QED systems to simulate such physical models relies on the successful simulation of Jahn-Teller (JT) interactions [6–8] which require atom-photon ultrastrong coupling conditions [9].

JT models describe the interaction of localized electronic states with vibrational (phonon) modes in crystals or in molecules [10]. Cavity QED systems that simulate single-mode JT models have been already proposed [11]. On the other hand, many practical systems need a description in terms of multimode JT interactions [12–16]. We address the question of how to generalize the restrictive single-mode simulation of JT systems to two-mode JT interactions within the circuit QED context.

Circuit QED [17] offers the possibility of operating in the ultrastrong coupling regime [18–23] for efficient JT and related spin-boson or Dicke model simulations. Photonic waveguide arrays are alternatively proposed [24] for reaching the deep ultrastrong coupling regime (DSC) [25] of JT-type light-matter interaction.

Our idea is to consider a system consisting of a two-level atom simultaneously interacting with two cavities coupled to each other, rather than with a degenerate two-mode cavity, which was considered for the cylindrically symmetric $E \times \epsilon$ JT model in cavity QED [11]. In terms of the normal modes of the coupled cavities, our system allows the simulation of a two-frequency (two nondegenerate vibrational normal modes) $E \times (\beta_1 + \beta_2)$ JT model [10]. The normal modes of the two coupled cavities consist of a high-frequency component and a low-frequency component. The coupling strength between the cavities can be utilized to alter the frequency ratio of the modes to simulate different frequency ratios encountered in different JT impurities in solids [26]. In addition to more realistic simulations of JT systems, establishing a link between multimode JT models and coupled circuit QED systems could enable the exploration of many-body physics, such as quantum chaos [13,14], quantum phase transitions [15], and quantum entanglement in JT systems [23,27], by using coupled cavity arrays.

We consider a coupled circuit QED [17,28–32] system in the ultrastrong coupling regime as a feasible platform on which to realize our idea. The system consists of two coupled lumped-element *LC* resonators interacting with a two-level artificial atom, a superconducting flux qubit. In the ultrastrong coupling regime the rotating-wave approximation is not valid, so that the qubit-resonator coupling is of JT type rather than Jaynes-Cummings type [21,23], allowing strongly coupled multifrequency JT systems to be simulated. The switchable ultrastrong coupling architecture can also be applied if a tunable coupling strength between the resonators and the flux qubit is desired [33].

Typical treatments of strongly coupled multimode JT systems in chemistry or in condensed matter physics utilize a cluster model [34] or use an effective single-mode model where most of the JT interaction energy is concentrated predominantly upon a single effective vibrational frequency with a negligible spread (narrow range of frequencies) [35]. These methods are especially used for interpreting effects associated with low energy states, such as those seen in low-temperature optical absorption [36].

When the frequency difference between the two modes is large, the situation is analogous to the case of optical and acoustic phonons in solids for which perturbative corrections become significant. We show that the frequency separation of the modes over which the JT interaction is distributed can be tuned with the coupling strength between the resonators. Our coupled circuit QED proposal allows for systematic simulation of effective single-mode and pure two-mode effects as well as transitions between these regimes.

This manuscript is organized as follows. In Sec. II we introduce the two-mode JT model and its implementation in a circuit QED context. The effective single-mode treatment is described

*omustecap@ku.edu.tr

in Sec. III. In Sec. IV, the experimental implementation is laid out. The results and discussions are presented in Sec. V. Finally, we give conclusions in Sec. VI.

II. TWO-FREQUENCY JT SYSTEMS IN CAVITY AND CIRCUIT QED

When two electronic levels are coupled to vibrations of ions or atoms in solids and molecules, the general form of the interaction can be written as $H_{\rm JT} = \vec{f}(Q)\cdot\vec{\sigma}$, where $\vec{f}(Q)$ is a vector valued function of vibrational coordinates while $\vec{\sigma}$ is the vector of the Pauli spin matrices. Such interactions are in general called Jahn-Teller interactions [10]. In this paper, we focus on a particular one of the form $(Q_{1x}+Q_{2x})\sigma_x$, which is known as the $E\times(\beta_1+\beta_2)$ JT (or Herzberg-Teller) model. Our aim is to generalize the recently discussed simulation of the single-mode $E\times\epsilon$ JT model in cavity QED [11,37], which is of the form $Q_x\sigma_x + Q_y\sigma_y$, to the two-frequency case. Our choice of $E\times(\beta_1+\beta_2)$ is the simplest possible two-frequency JT model. The implementation of $E\times(\beta_1+\beta_2)$ model allows the simulation of realistic crystals that exhibit spatial anisotropy. The single-boson $E\times\beta$ model is formally equivalent to the Dicke model, and signatures of quantum chaos have been discussed in the $E\times(\beta_1+\beta_2)$ model recently [15].

The Hamiltonian corresponding to the multifrequency JT interaction between a single impurity ion and many vibrational degrees of freedom of the host lattice (or molecule) is expressed as

$$H = H_{\rm ph} + H_{\rm JT}, \tag{1}$$

where $H_{\rm ph}$ describes the free Hamiltonian of the phonon modes at frequencies ω_i

$$H_{\rm ph} = \sum_i \hbar\omega_i(\hat{a}_i^\dagger\hat{a}_i), \tag{2}$$

where $\hat{a}_i(\hat{a}_i^\dagger)$ are the annihilation (creation) operators of the phonons. The multi-mode JT interaction describes the coupling of the single ion to the vibrational modes

$$H_{\rm JT} = \sum_i \hbar\omega_i k_i(\hat{a}_i + \hat{a}_i^\dagger)V. \tag{3}$$

Here k_i are the dimensionless scaling factors of the JT coupling coefficients and V is an operator that depends on the electronic degrees of freedom of the impurity ion.

We wish to simulate this multimode JT interaction using a coupled two-resonator circuit QED system. Normal modes of the coupled microwave photons play the role of phonons, while a flux qubit plays the role of the impurity ion. The interaction of the flux qubit in the two-resonator circuit QED system mimics the local (short-range) interaction of the ion-phonon coupling. On the other hand, there is an additional nonlocal (long-range) coupling between the resonator modes, describing hopping of photons between the resonators in the circuit QED system which mimics the coupling between the vibrational phonons. The coupled resonator model can be written as ($\hbar = 1$)

$$H = H_q + H_c + H_{qc} + H_{cc}, \tag{4}$$

where

$$H_q = \frac{\Omega}{2}\sigma_z, \tag{5}$$

$$H_c = \Omega_1\hat{\alpha}_1^\dagger\hat{\alpha}_1 + \Omega_2\hat{\alpha}_2^\dagger\hat{\alpha}_2, \tag{6}$$

$$H_{qc} = [\lambda_1(\hat{\alpha}_1^\dagger + \hat{\alpha}_1) + \lambda_2(\hat{\alpha}_2^\dagger + \hat{\alpha}_2)]\sigma_x, \tag{7}$$

$$H_{cc} = J(\hat{\alpha_1}^\dagger\hat{\alpha_2} + \hat{\alpha_2}^\dagger\hat{\alpha_1}), \tag{8}$$

where σ_z and $\sigma_x = \sigma_+ + \sigma_-$ are the Pauli spin operators describing the qubit degrees of freedom with Ω being the qubit transition frequency, $\Omega_{1,2}$ the resonance frequencies of the cavity modes, J the hopping rate of microwave photons between the resonators, and $\hat{\alpha}_{1,2}(\hat{\alpha}_{1,2}^\dagger)$ the annihilation (creation) operators for the cavity photons. We want to simulate the two-frequency JT model in Eq. (1) with the two-resonator circuit QED model in Eq. (4). For that aim it is necessary to be able to transform one model to the other and show that they are identical for a certain set of model parameters. In the next section we examine the transformation between these two Hamiltonians. We apply the so-called effective single privileged mode transformation that has been developed for multifrequency JT systems [35] that allows for systematic analysis of pure single- and multifrequency effects.

III. EFFECTIVE SINGLE-MODE JT SYSTEM IN TWO-RESONATOR CIRCUIT QED

We now employ the effective single-mode treatment [35] for the two-frequency JT model obtained within the two-resonator circuit QED context. Toward that aim, we look for a particular linear superposition of the normal modes of the coupled resonators,

$$\hat{\alpha}_i = \sum_k A_{ik}\hat{a}_k, \tag{9}$$

where A_{ik} are the elements of a real orthogonal matrix to be determined, such that most of the JT energy is concentrated over a privileged mode among the set of new bosonic modes $\hat{\alpha}_i$.

Without loss of generality, we choose the privileged mode as $\hat{\alpha}_1$ for which the single-mode model JT system can be written in terms of an effective frequency $\omega_{\rm eff}$ and an effective JT coupling $k_{\rm eff}$, scaled by $\omega_{\rm eff}$, so that

$$H_{\rm eff} = \frac{\Omega}{2}\sigma_z + \omega_{\rm eff}[\hat{\alpha}_1^\dagger\hat{\alpha}_1 + k_{\rm eff}(\hat{\alpha}_1 + \hat{\alpha}_1^\dagger)V]. \tag{10}$$

The relevant elements of the transformation, A_{11} and A_{12}, are determined by maximizing $k_{\rm eff}^2\omega_{\rm eff}$. This is the amount by which the minimum of the potential energy of the system is lowered, under adiabatic approximation, due to the interaction of the rest of the system with such a single mode [35]. This gives $A_{11} : A_{12} = k_1 : k_2$, subject to normalization conditions. Direct substitution of Eq. (9) into Eq. (1) yields

$$\omega_{\rm eff} = \frac{\omega_1 k_1^2 + \omega_2 k_2^2}{k_{\rm eff}^2}, \tag{11}$$

$$k_{\rm eff}^2 = k_1^2 + k_2^2. \tag{12}$$

For a 2×2 orthogonal matrix A, determining the first row of elements fixes the remaining two by orthonormality conditions such that

$$A = \frac{1}{k_{\text{eff}}} \begin{pmatrix} k_1 & k_2 \\ k_2 & -k_1 \end{pmatrix}, \tag{13}$$

which is taken in consistency with Ref. [35]. Such transformations are common in Morris-Shore bright- and dark-state transformations [38].For the system analyzed here, on the contrary, there is no perfect decoupling of either mode from the dynamics of the rest of the system, though for certain parameter regimes the modes $\hat{\alpha}_1$ and $\hat{\alpha}_2$ become approximately decoupled. The total transformed Hamiltonian can be written as

$$\tilde{H}_{\text{sys}} = H_{\text{eff}} + H'_{\text{ph}} + H_{\text{int}}, \tag{14}$$

where

$$H'_{\text{ph}} = \omega' \hat{\alpha}_2^\dagger \hat{\alpha}_2 \tag{15}$$

with

$$\omega' = \frac{\omega_1 k_2^2 + \omega_2 k_1^2}{k_{\text{eff}}^2} \tag{16}$$

is the free Hamiltonian of the disadvantaged effective mode. The interaction of this mode with the rest of the system is described by

$$H_{\text{int}} = c_2[(\hat{\alpha}_1^\dagger \hat{\alpha}_2 + \hat{\alpha}_1 \hat{\alpha}_2^\dagger) + k_{\text{eff}}(\hat{\alpha}_2 + \hat{\alpha}_2^\dagger)V]. \tag{17}$$

Here the strength of the coupling between the privileged and the disadvantaged modes is characterized by the parameter

$$c_2 = \Delta \frac{k_1 k_2}{k_{\text{eff}}^2}, \tag{18}$$

where $\Delta = \omega_1 - \omega_2$ is the frequency difference between the vibration modes in the two-frequency JT model. If the vibrational modes are degenerate, the model is exactly equivalent to the case of an effective single frequency. The coupling between the JT vibration modes can also be expressed as $c_2^2 = \overline{\omega^2} - \overline{\omega}^2$, where

$$\overline{\omega^n} = \frac{\omega_1^n k_1^2 + \omega_2^n k_2^2}{k_1^2 + k_2^2}. \tag{19}$$

This allows for interpreting c_2 as the mean square width of that distribution with a mean $\overline{\omega} = \omega_{\text{eff}}$ [35].

The effect of H_{int} on the effective single-mode model can be examined perturbatively provided that the frequency spread (Δ or c_2) is not too large. Perturbative effects will only be significant on the JT ground state starting from second order. To see this it is convenient to introduce a new set of operators [35]

$$\hat{\eta} = \hat{\alpha}_1 + k_{\text{eff}} V, \tag{20}$$

for which we can reexpress the effective model as

$$H_{\text{eff}} = \omega_{\text{eff}} \hat{\eta}^\dagger \hat{\eta} - \omega_{\text{eff}} k_{\text{eff}}^2 V^2. \tag{21}$$

The last term is proportional to the unit matrix. $\hat{\eta}$ obeys bosonic commutation rules even though it contains Pauli spin operators. This operator can be identified as a "bright" qubit-polariton quasiparticle. The first term in the effective Hamiltonain is then a harmonic oscillator contribution due to the free energy of these quasiparticles. The interaction Hamiltonian becomes

$$H_{\text{int}} = c_2(\hat{\eta}\hat{\alpha}_2^\dagger + \hat{\eta}^\dagger \hat{\alpha}_2), \tag{22}$$

representing the coupling of a bright qubit-polariton to a "dark" effective mode $\hat{\alpha}_2$. Using commutation relations between H_{eff} and $\hat{\alpha}_1$, the necessary matrix elements of $\hat{\eta}$ for the perturbation analysis in the representation of eigenstates of H_{eff} can be determined [35]. The simple relation $[H_{\text{eff}}, \hat{\alpha}_1] = -\omega_{\text{eff}} \hat{\eta}$ shows that $\hat{\eta}$ has no diagonal elements. This means that the perturbative corrections can only be of significance starting from second order, at least for the JT ground state and for low energy lying states. If the frequency spread c_2 is not negligible compared to the Jahn-Teller coupling k_{eff}, the description of the system using a privileged single mode is not possible since the JT energy is spread among the two modes $\hat{\alpha}_1, \hat{\alpha}_2$.

We are now in a position to relate the two-resonator circuit QED model of Eq. (4) to the two-frequency JT model of Eq. (1). We find that the parameters of the Hamiltonians are related as follows:

$$\omega_{\text{eff}} = \Omega_1, \quad \omega' = \Omega_2, \quad \omega_{\text{eff}} k_{\text{eff}} = \lambda_1, \quad c_2 k_{\text{eff}} = \lambda_2, \quad c_2 = J. \tag{23}$$

The relations require that a condition of the form

$$\Omega_1 = \frac{\lambda_1}{\lambda_2} J, \tag{24}$$

should be satisfied among the parameters of the circuit QED Hamiltonian.

IV. EXPERIMENTAL IMPLEMENTATION

The system we consider to implement the Hamiltonian in Eq. (4) consists of two lumped-element LC resonators capacitively coupled to each other and a flux qubit simultaneously coupled to each resonator. A schematic of the circuit can be seen in Fig. 1. The resonator-resonator interaction J is determined by the coupling capacitor C_c between the two LC resonators when they are in the ground state $J \simeq C_c V_{\text{rms}_1} V_{\text{rms}_2} = C_c \sqrt{\frac{\omega_1 \omega_2}{4 C_1 C_2}}$, where $C_{1,2}$ is the total capacitance of the uncoupled resonators. Using typical sample parameters [19,28], the coupling strength between the two resonators can be made very large, up to a considerable fraction of the frequency of each resonator. The spurious inductive resonator-resonator coupling could be minimized with an appropriate resonator geometry, if necessary. The flux qubit can also be made of large enough size (as the ones in Ref. [39]) so as to increase the distance between the resonators and reduce the mutual resonator-resonator inductance.

The coupling energy λ in a flux qubit-resonator system can become a large fraction of the energy of the resonator if the qubit is galvanically attached to the resonator, as already demonstrated experimentally in Refs. [18,19]. For a qubit either sharing a long section of its inductance [19] or a Josephson junction [18,21] with a resonator, coupling energies $\lambda \approx \omega_{1,2}$ are within reach experimentally.

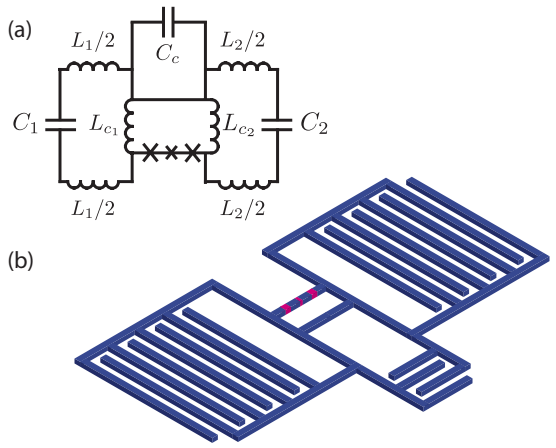

FIG. 1. (Color online) (a) Schematic of a flux qubit galvanically coupled to two LC resonators through coupling inductances $L_{c_{1,2}}$. Each resonator has resonant frequency $\omega_{1,2} = [(L_{1,2} + L_{c_{1,2}})C_{1,2}]^{-1/2}$. The resonators are coupled to each other through the coupling capacitor C_c. (b) Implementation of the circuit using interdigitated finger capacitors. Feed lines individually coupled to each resonator can be employed to probe the internal photon state of the resonators.

From the analysis of Sec. III, in order to study the privileged mode regime the coupling term in Eq. (10) needs to be larger than the coupling term in Eq. (17). This implies, according to the relations in Eq. (23), that $\lambda_1 > \lambda_2, J$. Therefore, in the experiment the flux qubit has to be ultrastrongly coupled to one resonator and strongly coupled to the other resonator, while the resonator-resonator coupling must be close to the qubit-resonator strong coupling. These designed coupling energies will determine the privileged mode. Detecting the photon state of each resonator using feed lines [40] permits the exploriation of the spectral properties of the complete system.

V. RESULTS

For the sake of simplicity, we choose $k_1 = k_2 = k$ so that $k_{eff} = \sqrt{2}k$. The relations in Eq. (23) reduce to $\Omega_1 = \Omega_2 \equiv \Omega_c = (\omega_1 + \omega_2)/2, \lambda_1 = (\omega_1 + \omega_2)k/\sqrt{2}, \lambda_2 = \Delta k/\sqrt{2}$ and $J = c_2 = \Delta/2$. Our choice requires the resonators in the circuit QED system to be degenerate. We further assume resonance condition $\Omega = \Omega_c$. The circuit QED Hamiltonian then becomes

$$H = \hat{\alpha}_1^\dagger \hat{\alpha}_1 + \hat{\alpha}_2^\dagger \hat{\alpha}_2 + \frac{1}{2}\sigma_z + \frac{\Delta}{2}(\hat{\alpha}_1^\dagger \hat{\alpha}_2 + \hat{\alpha}_2^\dagger \hat{\alpha}_1) + k_{\text{eff}}\left((\hat{\alpha}_1^\dagger + \hat{\alpha}_1) + \frac{\Delta}{2}(\hat{\alpha}_2^\dagger + \hat{\alpha}_2)\right)\sigma_x. \quad (25)$$

We use dimensionless energy and time, scaled by $\hbar\Omega_c$ and $1/\Omega_c$, respectively, but do not change our notation for scaled variables. Our model is then a two-parameter (k, Δ) theory where Δ is in units of Ω_c.

The resonators are degenerate but the system still simulates the two-frequency JT model. The coupling coefficient between the resonators J determines the frequency ratio of the two vibration modes in the corresponding two-frequency JT Hamiltonian of Eq. (1) to be simulated, which becomes

$$H = \omega_1 \hat{a}_1^\dagger \hat{a}_1 + \omega_2 \hat{a}_2^\dagger \hat{a}_2 + \tfrac{1}{2}\sigma_z + k[\omega_1(\hat{a}_1^\dagger + \hat{a}_1) + \omega_2(\hat{a}_2^\dagger + \hat{a}_2)]\sigma_x, \quad (26)$$

where the frequency ratio is determined by

$$\frac{\omega_1}{\omega_2} = \frac{1 + \Delta/2}{1 - \Delta/2}. \quad (27)$$

Some cases of interest are the 2:1 frequency ratio of the two phonon modes in $C_6H_6^{\pm}$ and the frequency ratio 3:1 of the two phonon modes of Fe^{2+} in ZnS [26]. As explained in Sec. III, the transformation or equivalence of these two Hamiltonians is exact. For Δ (or the frequency spread c_2) small compared to the uncoupled eigenfrequencies of the qubit and the resonators, we obtain a faithful representation of the two-frequency JT model in terms of the privileged mode. Corrections appear only as second-order perturbations.

We first examine the eigenenergies of the Hamiltonian in Eq. (25). The lowest five eigenvalues are shown in Fig. 2. Here the Fock space dimension for each resonator mode is fixed to 2 so that we consider up to two-photon manifolds. We examined the influence of dimensions of the Fock space on our results in the case of spectrum calculations and found them to be sufficiently robust. The strong coupling case with $k = 0.1/\sqrt{2}$ (or just the beginning of the ultrastrong coupling regime) is considered in Fig. 2(a). When $\Delta = 0$ there is only pure Rabi splitting, as can be seen in the first excited level. When Δ increases, the coupling between the privileged and the disadvantaged modes increases. This polaritonic interaction of the modes causes further repelling of the Rabi-split levels. Single privileged effective mode description of the system would only be valid over a narrow band $k \sim |\Delta| < 0.1$. The ultrastrong coupling regime with $k = 1/\sqrt{2}$ is considered in Fig. 2(b). An asymmetric Rabi splitting at $\Delta = 0$ can be seen in the first excited level. Here the effective single-mode description is valid over a broader range $|\Delta| < 1$. The dependence of the energy spectrum on the full range of k and Δ is shown in Fig. 2(c). The first band is tent-shaped, and for low k it varies sharply with Δ resulting in a narrow regime of the effective single-mode description. As k reaches ultrastrong coupling conditions, the regime of effective single-mode description becomes more robust against variations in Δ over a broader range.

Solid-state and molecular multi-frequency JT systems are usually investigated through their absorption spectrum. The corresponding quantity in circuit QED is the transmission spectrum of the resonators. We consider the power spectrum of only one resonator, corresponding to the privileged mode. Deviations from single-mode behavior in this spectrum would be identified as pure two-frequency effects. In order to calculate the power spectrum it is necessary to solve the quantum master equation for the ultrastrong coupling regime, which can only be rigorously formulated in the dressed state picture of coupled qubit-resonator, examined recently in Refs. [41,42]. Our purpose is to see qualititative changes in the spectrum at different frequency ratios of the two-frequency JT model. We assume that the usual Bloch-Redfield quantum

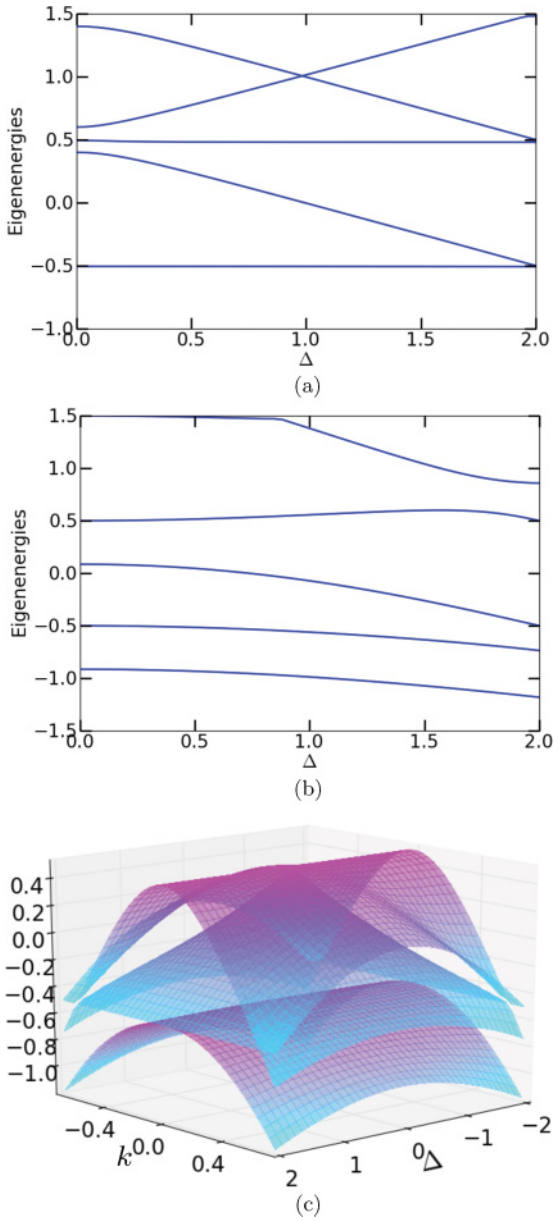

FIG. 2. (Color online) Dependence of the lowest five eigenenergies of the two-frequency Jahn-Teller model on the mode-coupling parameter Δ. (a) For the qubit-cavity coupling scaling parameter $k = 0.1/\sqrt{2}$, the splitting of the first energy level into three at $\Delta = 0$ is a pure Rabi splitting. The privileged effective single-mode regime is valid over a narrow band $|\Delta| < 0.1$. (b) At $k = 1/\sqrt{2}$ the energy-level transitions become flat over a broader band $|\Delta| < 1$, deeper into the ultrastrong coupling regime. (c) Energy bands of the two-frequency Jahn-Teller model depending on the mode-coupling parameter Δ and the qubit-cavity coupling scaling parameter k. All the quantities plotted are dimensionless as explained in the text.

master equation for circuit QED systems in the Born-Markov approximation is applicable for our purposes [40], and the equation is given as ($\hbar = 1$)

$$\frac{d\rho}{dt} = -i[H,\rho] + \mathcal{L}\rho, \tag{28}$$

where the Liouvillian superoperator $\mathcal{L}$ is given by

$$\mathcal{L}\rho = \sum_{j=1,2}(1+n_{\rm th})\kappa\mathcal{D}[\hat{\alpha}_j]\rho + n_{\rm th}\kappa\mathcal{D}[\hat{\alpha}_j^\dagger]\rho + \gamma\mathcal{D}[\sigma]\rho + \frac{\gamma_\phi}{2}\mathcal{D}[\sigma_z]\rho, \tag{29}$$

with $n_{\rm th}$ being the average thermal photon number, which we take as $n_{\rm th} = 0.1$ corresponding to 100 mK [40]. The Lindblad-type damping superoperators are denoted by $\mathcal{D}$. The cavity photon loss rate κ is taken to be the same for both resonators. The qubit relaxation and dephasing rates are represented by γ and γ_ϕ, respectively.

The JT spectrum is determined by calculating the real part of the Fourier transform of the stationary two-time first-order correlation function for the privileged mode $\hat{\alpha}_1$, so that

$$P(\omega) = \int_{-\infty}^{\infty}\langle\hat{\alpha}_1^\dagger(t)\hat{\alpha}_1(0)\rangle e^{-i\omega t}. \tag{30}$$

We use Python programming language with the QuTip package for the determination of the spectrum [43]. The decay parameters, scaled by Ω_c, are taken to be $\kappa = 0.001, \gamma = 0.001$, and $\gamma_\phi = 0.01$, while assuming Fock space of up to two photons for each resonator mode. When we consider higher Fock space dimensions (due to numerical constraints we examined up to five particle manifolds), we find that the spectrum is robust against the variations in the Fock space dimensions for the regimes of $J \leqslant 0.5$ we consider. At larger J values small changes in the spectral intensities are observed, but they are still negligible up to $J \sim 1$. For smaller decay rates and at even larger J values the spectrum becomes more sensitive to dimensions of the Fock space.

Our results for different values of J are presented in Fig. 3. Figure 3(a) shows the spectrum when the two resonators are uncoupled, $J = 0$. For low $k_{\rm eff}$, the spectrum shows typical asymmetric Rabi-split frequency peaks of the Jaynes-Cummings (JC) model around the degenerate frequency of the resonators. At larger values of $k_{\rm eff} \sim 1$ the system is in the single-mode JT regime. Figure 3(b) presents the effect of coupling the resonators with $J = 1/2$, which corresponds to the typical frequency ratio 3:1 of two phonon modes of Fe^{2+} in ZnS. The polaritonic splitting here shifts the Rabi-split peaks farther away at low values of $k_{\rm eff}$. For $k_{\rm eff} \sim 1$ the system is in the two-mode JT regime. Figure 3(c) shows similar features for $J = 1/3$, which corresponds to the typical value of frequency ratio 2:1 of the two phonon modes in $C_6H_6^{\pm}$. In this case for $k_{\rm eff} > 1.5$ the system enters the effective single-mode JT regime.

The general behavior of the spectrum with the resonator-resonator coupling J at a given qubit-resonator coupling $k_{\rm eff}$ is shown in Fig. 4. Figure 4(a) shows the case when k is near the threshold of the ultrastrong coupling regime, $k_{\rm eff} = 0.1$. The spectrum is mainly determined by the two-frequency character of the system, corresponding to the two-mode Jaynes-Cummings model. The privileged single-mode description is limited to very small coupling strengths $J = \Delta/2 \lesssim 0.1$. Beyond this point, normal mode splitting increases with J.

When we consider the case of deeper ultrastrong coupling $k_{\rm eff} = 1$, Fig. 4(b) reveals that it is easier to resolve the single-mode and two-moderegimes as the single-mode regime

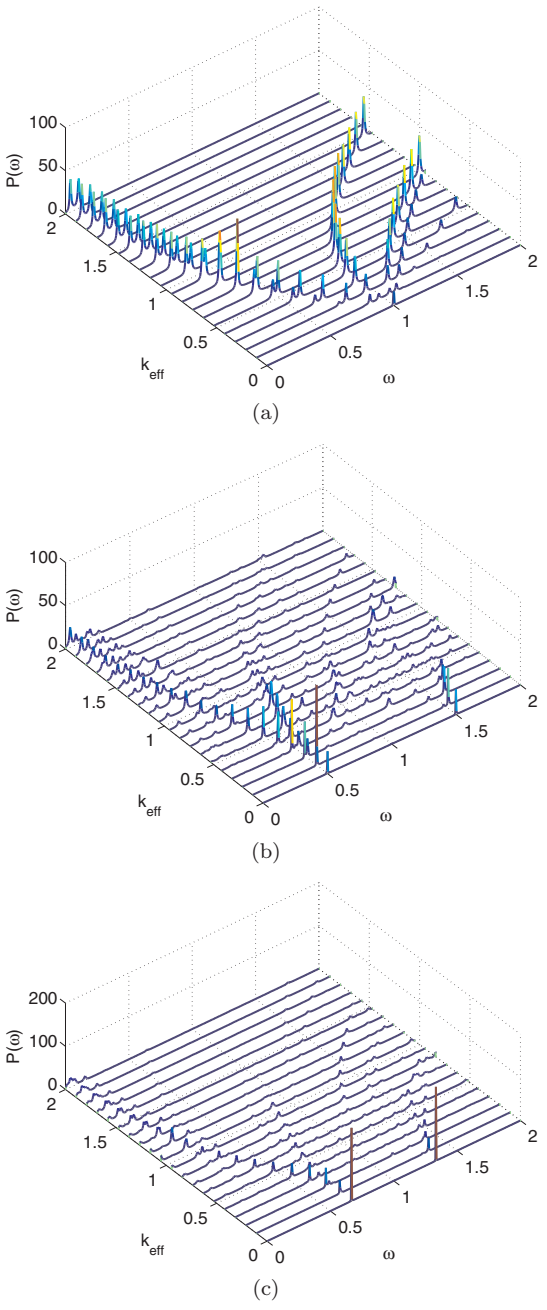

FIG. 3. (Color online) Resonator-qubit coupling k_{eff} dependence of the cavity emission spectrum for the privileged effective mode in the two-frequency Jahn-Teller model for different values of the resonator-resonator coupling strength J. (a) $J = 0$ corresponds to the pure single-mode regime. $k_{\text{eff}} \ll 1$ is the single-mode regime in the JC model. For $k_{\text{eff}} \gtrsim 1$ one enters the regime of single-mode JT model. (b) $J = 1/2$ shows three regimes: $k_{\text{eff}} \ll 1$ (two-mode JC model), $k_{\text{eff}} \gtrsim 1$ (two-mode JT model), and $k_{\text{eff}} \gg J$ (effective single-mode JT model). This case simulates the frequency ratio of 3:1 of the two phonon modes in Fe^{2+} in ZnS. (c) $J = 1/3$ simulates the frequency ratio of 2:1 of the two phonon modes in $C_6H_6^{\pm}$. In this case the effective single-mode regime is more clear for $k_{\text{eff}} > 1.5$.

is significantly enhanced, up to $J = \Delta/2 \sim 0.4 < k_{\text{eff}}$. This observation complies with our previous arguments, based upon the energy levels of the system in Fig. 3. Beyond the

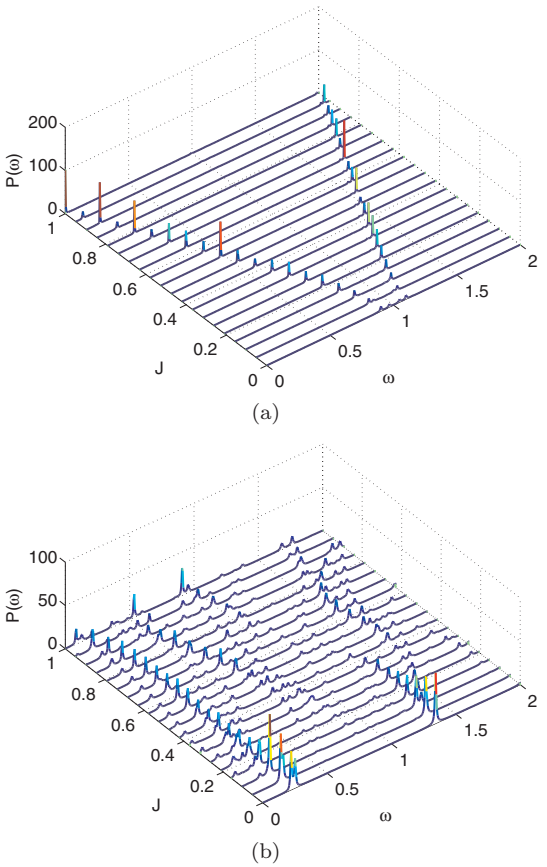

FIG. 4. (Color online) Variation of cavity emission spectrum for the privileged effective mode in the two-frequency Jahn-Teller model with resonator-resonator coupling J at (a) $k_{\text{eff}} = 0.1$ and (b) $k_{\text{eff}} = 1$.

single-mode regime, Fig. 4(b) shows that the higher frequency peak at $\omega \sim 1.4$ disappears, while the lower frequency one at $\omega \sim 0.2$ dominates. The spectrum exhibits additional peaks that grow in number and in amplitude in the two-frequency regime. These peaks are due to multiphoton processes that become more and more significant as one goes deeper into the strongly coupled JT model [44]. The higher energy resonance in the single-mode regime turns out to be more susceptible to such multiphoton processes. The amplitude of this transition decreases and eventually vanishes in the two-frequency regime, while the lower energy resonance is more robust and does not decrease its amplitude significantly. These results suggest that one can monitor and analyze the transition between the effective single privileged mode and the pure two-frequency behavior of a JT system by tuning the circuit QED parameters into the DSC regime.

VI. CONCLUSIONS

In summary, we have presented a method to simulate a two-frequency JT model by using a two-resonator circuit QED system. The proposed model consists of a flux qubit coupled to two resonators in the ultrastrong coupling regime. An exact transformation between the two-frequency JT Hamiltonian and the circuit QED Hamiltonian has been established. The transformation permits describing the system in terms of an effective privileged single mode under certain conditions of the

control parameters of the circuit QED system. The effective disadvantaged mode can be decoupled from the privileged one in the ultrastrong coupling regime. The eigenenergy spectrum and power spectrum are calculated using ultrastrong circuit QED parameters, with specific attention to the present experimental restrictions. The tunability of the pure two-mode JT model and the effective privileged mode model is found to be feasible in the ultrastrong coupling circuit QED within the range of parameters in present experiments.

Simulating and interpreting more complex JT systems, such as vacancies in graphite or fullerides C_{60}^{-}, would require going beyond a two-mode description. Our analysis of the two-frequency JT model simulation can serve as a building block for further realizations of other classes of multimode JT systems, by considering, for example, coupled multimode superconducting transmission line resonators and their interactions with flux qubits in the (ultra)strong coupling regime. Such extensions of the present work would allow examining rich geometric phase effects [37] and designing synthetic gauge fields, as well as enhancing the comprehension of nonlinear JT dynamics of complex molecular systems.

ACKNOWLEDGMENTS

We acknowledge inspiring comments by D. Ballester and M. Mariantoni. P. F.-D. acknowledges funding by the Institute for Quantum Information and Matter, an NSF Physics Frontier Center with support of the Gordon and Betty Moore Foundation, by NSF Grant No. PHY0652914, by the DoD NSSEFF program, by the AFOSR MURI for Quantum Memories, and by Northrop Grumman Aerospace Systems. This work is supported by D.P.T. (T.R. Prime Ministry State Planning Organization) under Project No. 2009K12020 and by National Science Foundation of Turkey under Project No. 109T267 and Project No. 111T285. Y. G. gratefully acknowledges support by TÜBİTAK Post-Doc Program.

[1] M. Lewenstein *et al.*, *Traveling to Exotic Places With Ultracold Atoms*, AIP Conference Proceedings, Vol. 869 (American Institute of Physics, Melville, 2006), pp. 201–211.
[2] H. T. C. Stoof, E. Vliegen, and U. Al Khawaja, Phys. Rev. Lett. **87**, 120407 (2001).
[3] L. J. Garay, J. R. Anglin, J. I. Cirac, and P. Zoller, Phys. Rev. Lett. **85**, 4643 (2000).
[4] M. Johanning, A. Varûn, and C. Wunderlich, J. Phys. B **42**, 154009 (2009).
[5] J. Larson, Phys. Scr. T **140**, 014025 (2010).
[6] D. R. Yarkony, Rev. Mod. Phys. **68**, 985 (1996).
[7] C. A. Mead, Rev. Mod. Phys. **64**, 51 (1992).
[8] A. Bohm, A. Mostafazadeh, H. Koizumi, Q. Niu, and J. Zwanziger, *The Geometric Phase in Quantum Systems: Foundations, Mathematical Concepts, and Applications in Molecular and Condensed Matter Physics* (Springer, Berlin, 2003).
[9] C. Ciuti and I. Carusotto, Phys. Rev. A **74**, 033811 (2006).
[10] I. Bersuker and I. Bersuker, *The Jahn-Teller Effect* (Cambridge University Press, Cambridge, 2006).
[11] J. Larson, Phys. Rev. A **78**, 033833 (2008).
[12] R. S. Markiewicz and C. Kusko, Phys. Rev. B **66**, 024506 (2002).
[13] E. Majerníková and S. Shpyrko, Phys. Rev. E **73**, 057202 (2006).
[14] E. Majerníková and S. Shpyrko, Phys. Rev. E **73**, 066215 (2006).
[15] E. Majerníková and S. Shpyrko, J. Phys. A: Math. Theor. **44**, 065101 (2011).
[16] M. Eva and S. Serge, J. Phys. A **44**, 065101 (2011).
[17] A. Wallraff *et al.*, Nature (London) **431**, 162 (2004).
[18] T. Niemczyk *et al.*, Nature Phys. **6**, 772 (2010).
[19] P. Forn-Díaz, J. Lisenfeld, D. Marcos, J. J. García-Ripoll, E. Solano, C. J. P. M. Harmans, and J. E. Mooij, Phys. Rev. Lett. **105**, 237001 (2010).
[20] M. H. Devoret, S. M. Girvin, and R. J. Schoelkopf, Ann. Phys. (Leipzig) **16**, 767 (2007).
[21] J. Bourassa, J. M. Gambetta, A. A. Abdumalikov, O. Astafiev, Y. Nakamura, and A. Blais, Phys. Rev. A **80**, 032109 (2009).
[22] D. Ballester, G. Romero, J. J. García-Ripoll, F. Deppe, and E. Solano, Phys. Rev. X **2**, 021007 (2012).
[23] C. P. Meaney, T. Duty, R. H. McKenzie, and G. J. Milburn, Phys. Rev. A **81**, 043805 (2010).
[24] A. Crespi, S. Longhi, and R. Osellame, Phys. Rev. Lett. **108**, 163601 (2012).
[25] J. Casanova, G. Romero, I. Lizuain, J. J. García-Ripoll, and E. Solano, Phys. Rev. Lett. **105**, 263603 (2010).
[26] B. Halperin and R. Englman, Phys. Rev. B **9**, 2264 (1974).
[27] L. K. McKemmish, R. H. McKenzie, N. S. Hush, and J. R. Reimers, J. Chem. Phys. **135**, 244110 (2011).
[28] I. Chiorescu *et al.*, Nature (London) **431**, 159 (2004).
[29] G. M. Reuther, D. Zueco, F. Deppe, E. Hoffmann, E. P. Menzel, T. Weissl, M. Mariantoni, S. Kohler, A. Marx, E. Solano, R. Gross, and P. Hanggi, Phys. Rev. B **81**, 144510 (2010).
[30] M. Mariantoni, F. Deppe, A. Marx, R. Gross, F. K. Wilhelm, and E. Solano, Phys. Rev. B **78**, 104508 (2008).
[31] M. Mariantoni, H. Wang, R. C. Bialczak, M. Lenander, E. Lucero, M. Neeley, A. D. O'Connell, D. Sank, M. Weides, J. Wenner, T. Yamamoto, Y. Yin, J. Zhao, J. M. Martinis, and A. N. Cleland, Nat. Phys. **7**, 287 (2011).
[32] H. Wang, M. Mariantoni, R. C. Bialczak, M. Lenander, E. Lucero, M. Neeley, A. D. O'Connell, D. Sank, M. Weides, J. Wenner, T. Yamamoto, Y. Yin, J. Zhao, J. M. Martinis, and A. N. Cleland, Phys. Rev. Lett. **106**, 060401 (2011).
[33] B. Peropadre, P. Forn-Diaz, E. Solano, and J. J. Garcia-Ripoll, Phys. Rev. Lett. **105**, 023601 (2010).
[34] J. Van Vleck, J. Chem. Phys. **7**, 72 (1939).
[35] M. O'Brien, J. Phys. C **5**, 2045 (1972).
[36] J. Fletcher, M. O'Brien, and S. Evangelou, J. Phys. A: Math. Gen. **13**, 2035 (1980).
[37] J. Larson, E. Nour Ghassemi, and A. Larson, arXiv:1111.4647.
[38] J. R. Morris and B. W. Shore, Phys. Rev. A **27**, 906 (1983).
[39] T. Hime, P. A. Reichardt, B. L. T. Plourde, T. L. Robertson, C.-E. Wu, and A. V. Ustinov, and J. Clarke, Science **314**, 1427 (2006).

[40] J. M. Fink, L. Steffen, P. Studer, L. S. Bishop, M. Baur, R. Bianchetti, D. Bozyigit, C. Lang, S. Filipp, P. J. Leek, and A. Wallraff, Phys. Rev. Lett. **105**, 163601 (2010).
[41] F. Beaudoin, J. M. Gambetta, and A. Blais, Phys. Rev. A **84**, 043832 (2011).
[42] J. Hausinger and M. Grifoni, New J. Phys. **10**, 115015 (2008).
[43] J. R. Johansson, P. D. Nation, and F. Nori, Comp. Phys. Comm. **183**, 1760 (2012).
[44] An equivalent result is obtained in the Jaynes-Cummings model beyond the rotating-wave approximation in M. H. Naderi, J. Phys. A: Math. Theor. **44**, 055304 (2011).